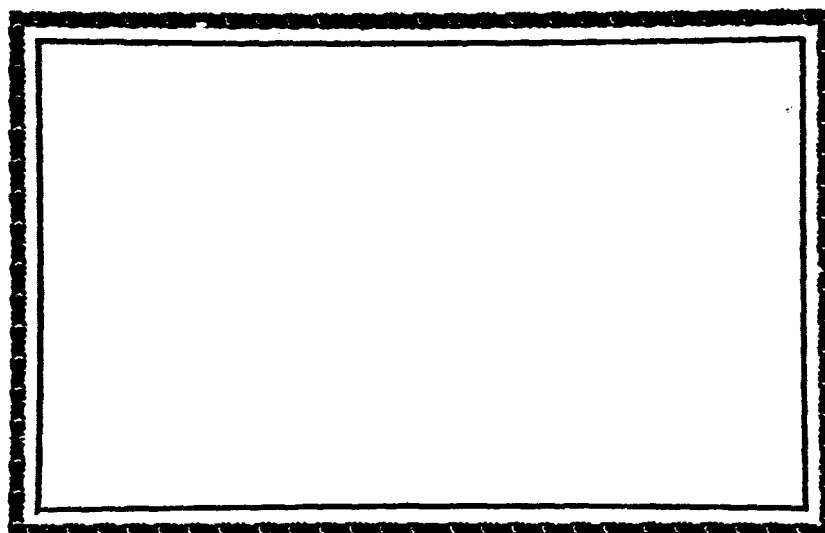


(NASA-CR-143041) RADIATIVE PROPERTY  
INVESTIGATION Final Report (Southern Univ.)  
55 p HC \$4.25 CSCL 11C

N75-26138

Unclas  
G3/27 27326



DEPARTMENT OF  
MECHANICAL ENGINEERING

SOUTHERN UNIVERSITY  
BATON ROUGE, LOUISIANA 70813

**FINAL REPORT**  
**ON NASA GRANT NSG-8016**  
**RADIATIVE PROPERTY INVESTIGATION**

**To**  
**National Aeronautics and Space Administration**

**Submitted by: Robert L. Scott Jr.**  
**Department of Mechanical Engineering**  
**Southern University, Baton Rouge, Louisiana**

## SUMMARY

Measurements of the bidirectional reflections of NASA paints Z-93 and S-13G were made for 0.5, 1.78, and 2.5 microns, source incidence angles of  $0^{\circ}$ ,  $30^{\circ}$ ,  $60^{\circ}$ , and  $75^{\circ}$ , and four detector azimuth positions. The apparatus used for the measurements was the one discussed in the final report of NASA Grant NGR-005-009.

The bidirectional reflectance distribution was found to be near Lambert for azimuth positions not too close to  $180^{\circ}$  from the source incident azimuth. The reflectance distribution at an azimuth of  $180^{\circ}$  from the source is close to Lambert for near normal source incident angles, and becomes much larger than Lambert as the source incident angle approaches grazing. The reflectance deviates from Lambert as the wavelength increases. Comparison of data for the paints shows Z-93 reflectance is much closer to Lambert than S-13G. When there is a peak in the reflectance distribution it occurred at the specular angle or an angle larger than the specular angle.

## Table of Contents

	Page
Summary.....	ii
Table of Contents.....	iii
List of Tables.....	v
List of Illustrations.....	vi
Introduction.....	i
Apparatus and Specimen Preparation.....	2
Presentation and Discussion of Results....	5
Appendix.....	53

**ORIGINAL PAGE IS  
OF POOR QUALITY**

# LIST OF TABLES

Table		Page
1.	Variation of Reflectance with Source and Detector Azimuth.....	26
2.	Reflectance of S-13G at 0.500 Microns $\psi = 0^\circ$ .....	27
3	Reflectance of S-13G at 1.78 Microns $\psi = 0^\circ$ .....	28
4	Reflectance of S-13G at 2.5 Microns $\psi = 0^\circ$ .....	29
5.	Reflectance of S-13G at 0.500 Microns $\psi = 30^\circ$ .....	30
6	Reflectance of S-13G at 1.78 Microns $\psi = 30^\circ$ .....	31
7	Reflectance of S-13G at 2.5 Microns $\psi = 30^\circ$ .....	32
8.	Reflectance of S-13G at 0.500 Microns $\psi = 60^\circ$ .....	33
9	Reflectance of S-13G at 1.78 Microns $\psi = 60^\circ$ .....	34
10.	Reflectance of S-13G at 2.5 Microns $\psi = 60^\circ$ .....	35
11.	Reflectance of S-13G at 0.500 Microns $\psi = 75^\circ$ .....	36
12.	Reflectance of S-13G at 1.78 Microns $\psi = 75^\circ$ .....	37
13.	Reflectance of S-13G at 2.5 Microns $\psi = 75^\circ$ .....	38
14.	Variation of Reflectance with Source Incident Angle - S-13G.....	39

# LIST OF TABLES (CONTINUED)

Table	Page
15. Reflectance of Z-93 at 0.500 Microns $\psi = 0^\circ$ .....	40
16. Reflectance of Z-93 at 1.78 Microns $\psi = 0^\circ$ .....	41
17. Reflectance of Z-93 at 2.5 Microns $\psi = 0^\circ$ .....	42
18. Reflectance of Z-93 at 0.500 Microns $\psi = 30^\circ$ .....	43
19. Reflectance of Z-93 at 1.78 Microns $\psi = 30^\circ$ .....	44
20. Reflectance of Z-93 at 2.5 Microns $\psi = 30^\circ$ .....	45
21. Reflectance of Z-93 at 0.500 Microns $\psi = 60^\circ$ .....	46
22. Reflectance of Z-93 at 1.78 Microns $\psi = 60^\circ$ .....	47
23. Reflectance of Z-93 at 2.5 Microns $\psi = 60^\circ$ .....	48
24. Reflectance of Z-93 at 0.500 Microns $\psi = 75^\circ$ .....	49
25. Reflectance of Z-93 at 1.78 Microns $\psi = 75^\circ$ .....	50
26. Reflectance of Z-93 at 2.5 Microns $\psi = 75^\circ$ .....	51
27. Variation of Reflectance with Source Incident Angle - Z-93 .....	52

## LIST OF ILLUSTRATIONS

Figure	Page
1. Specimen Holder and Installation Device.....	8
2. Specimen Installation .....	9
3. Schematic of Exit Optics.....	10
4. Reflectance of S-13G for $\phi = 90^\circ$ .....	11
5. Reflectance of S-13G for $\psi = 0^\circ$ .....	12
6. Reflectance of S-13G for $\psi = 30^\circ$ .....	13
7. Reflectance of S-13G for $\psi = 60^\circ$ .....	14
8. Reflectance of S-13G for $\psi = 75^\circ$ .....	15
9. Variation of Reflectance with $\psi$ for S-13G.....	16
10. Reflectance of Z-93 for $\phi = 90^\circ$ .....	17
11. Reflectance of Z-93 for $\psi = 0^\circ$ .....	18
12. Reflectance of Z-93 for $\psi = 30^\circ$ .....	19
13. Reflectance of Z-93 for $\psi = 60^\circ$ .....	20
14. Reflectance of Z-93 for $\psi = 75^\circ$ .....	21
15. Variation of Reflectance of Z-93 with $\psi$ .....	22

# LIST OF ILLUSTRATIONS (CONTINUED)

Figure		Page
16.	Variation of Reflectance with $\phi$ for S-13G, $\lambda = 0.500\mu$ .....	25
17.	Variation of Reflectance with $\phi$ for Z-93, $\lambda = 0.500\mu$ .....	24
18.	Variation of Reflectance with $\lambda$ for S-13G and Z-93.....	25
A1.	Photographs of Z-93: (a) 10K Magnification; (b) 1K Magnification....	54
A2.	Photographs of S-13G: (a) 10K Magnification; (b) 1K Magnification....	55



## Introduction

The bidirectional reflectance investigation reported is a continuation of NASA Grant NGR 19-005-009. In that report a summary of the theory involved in electromagnetic reflection and a discussion of some published papers on bidirectional reflectance are presented. The instrumentation system and an analysis of the errors involved in the measurements are also presented. The definitions of various angles and other quantities are also given.

The detector output is proportioned to the energy reflected from the paints. The data presented here is the ratio of the detector signal to the signal when the detector zenith is zero;

$$\rho_n(\psi, \zeta; \theta, \phi) = \frac{D(\psi, \zeta; \theta, \phi)}{D(\psi, \zeta; 0, \phi)}$$

Where

- $\psi$  = Source Zenith
- $\zeta$  = Source Azimuth
- $\theta$  = Detector Zenith
- $\phi$  = Detector Azimuth

With this presentation the data will obey the cosine law for a perfect diffuse surface.

### Apparatus and Specimen Preparation

The primary changes in the apparatus are the use of a larger scale recorder which simplifies the data taking process and the use of a larger lead sulfide detector which increases the output signal. Other changes include such items as, using a stiffer table for the experimental set up, and designing and constructing an improved device for holding and adjusting the bidirectional device.

A method for installing the specimen on the bidirectional device was developed. The specimen which is supplied by NASA on a thin aluminum disc, and the 1 inch diameter holder combined axial length must be 1.785 inches as shown in Figure 1. The specimen normal must also be parallel to the axis of the cylindrical holder.

The specimen holder (part A) and specimen installation device (part B) are shown in Figure 1. A specimen is installed by placing it in the recess of part B as shown in Figure 2. An adhesive is placed on the center of the specimen holder and the holder is placed on part B upside down. A small amount of adhesive is used so that no adhesive touch part B. After the adhesive is dry part B is removed. The data in Table 1, shows there

is little change in the signal when the specimen is rotated about its axis. This is a good indication that the specimen is parallel to the axis as it should be.

During the earlier part of the investigation signal fluctuation made it all but impossible to take data. A General Electric 18 AMP tungsten ribbon filament lamp was being used for the near infrared region when this problem occurred. This lamp was being used because it was supplied with the monochromator. After trying several of the lamps that were new and observing no improvement in the signal stability a sylvania coiled tungsten quartz lamp was tried. The data showed this lamp was very stable and had an output about twice that of the General Electric ribbon lamp.

A problem that occurs with the use of a grating monochromator as in this investigation is the monochromatic energy leaving the monochromator is partially polarized. To alleviate this problem quartz plates were installed in the exit beam to eliminate any polarization. When two plates are used as shown in Figure 3 there is very little shift in the beam due to refraction.

When filters are used as shown in Figure 3 refraction causes some error in the location of the beam on the specimen. To eliminate this source of error filters

were installed at the inlet to the monochromotor.

In addition to these changes an effort is being made to modify the apparatus so that absolute reflectance measurements can be made. Preliminary results shows there are considerable difficulty in obtaining an accurate measurements of the source. There are primarily two problems to overcome. One is the source signal is about three orders of magnitude larger than the signal reflected from the paints. The second problem is it is difficult to obtain a repeatable measurement of the source signal. The first problem can be overcome by using calibrated neutral density filters.

A very accurate method of obtaining a quantitative comparison of the bidirectional reflectance would be to obtain measurements relative to some choosen standard such as magneisum carbonate.

The specimens composition and scanning electron microscop photographs are given in the Appendix. The photographs were provided by Mr. Daniel W. Gates of NASA.

**ORIGINAL PAGE IS  
OF POOR QUALITY**

### Presentation and Discussion of Results

The results of this investigation are given in Figure 4 through 15 and Tables 2 through 28. Data were taken for  $\psi = 0, 30, 60, \text{ and } 75$ ;  $\zeta = 180$ ;  $\phi = 0, 90, 180$  and  $270$  degrees. Data were taken for  $\theta$  less than  $85$  degrees and as close as  $5^\circ$  to the source zenith for the Pbs (Lead Sulfide detector) and  $10^\circ$  to the source zenith for the PMT (Photomultiplier Detector). The wavelength at which data were taken are  $0.5, 1.78$  and  $2.5$  microns. In some instances, on the graphs, two scales for the ordiante are used.

At  $0.50$  and  $1.78$  microns more than adequate detector signal was available. But the signal at  $2.50$  microns was fairly weak and this data have the most scatter. From Figures 4, 5, 10, and 11 it can be seen there is little difference in the reflectance of the two paints for  $\psi = 0$ . For  $\psi = 30^\circ$ ,  $\phi = 0$  the data for S-13G is above the cosine curve while that for Z-93 is below the cosine curve. Another difference is the data for Z-93 at  $\psi = 30^\circ$  shows a backscatter phenomena while for S-13G the data is close to the cosine curve. For Z-93 the tendency to have backscatter above the cosine curve decreases and the forward scatter increases as  $\psi$  increases but not nearly as much as that

of S-13G. This is exemplified by Figures 7, 8, 13, and 14.

None of the data have distinguishable peaks except for Z-93 when  $\psi = 60^\circ$ . Such peaks usually occur for nonconductors when the surface roughness is of the order of the wavelength. The reflecting surface of S-13G could be detected to the extremely rough by the naked eye and Z-93 appeared to be smooth. All of the data shows as the wavelength increases or the source zenith increases the forward scatter becomes larger than the cosine law.

The primary usefulness of Figures 9 and 15 is comparing data of different source zenith angles. Also, if one checks reciprocity these curves may be used as discussed in the final report on NASA NGR 19-005-009.

Figures 7 and 8 for S-13G and Figures 13 and 14 for Z-93 shows that the maximum in the reflectance which occurs when  $\phi = 0^\circ$ ,  $\psi = 60^\circ$  and  $75^\circ$  is at an angle greater than the corresponding specular angle. For  $\psi = 60^\circ$  the off specular peak is at least  $10^\circ$ . Also for Figures 7, 8, and 14 data have been included for  $\phi = 0$  and  $\lambda = 1.00$  microns. The signal at 1.00 microns was suprisingly large which was probably due to the Quartz lamb as compared to the ribbon lamb discussed earlier.

Figure 6 and Table 7 show that for  $\psi = 30^\circ$  the maximum in reflectance for  $\psi = 0^\circ$  occurs not at an angle greater

than the specular angle but less than the specular angle.

The method of aligning the detectors is to set the source zenith  $\psi$ , then with a mirror (front surface) as the specimen the detector is positioned so that the source reflects off the mirror onto the detector thus locating the detector zenith  $\theta$  and azimuth  $\phi$ . The error involved is approximately 0.25 degrees, so the off specular maximum is not due to the error of alignment.

Figures 16 and 17 show the variation in reflectance with detector azimuth. These Figures show most of the change in reflectance as  $\phi$  varies occur between  $\phi = 0^\circ$  to  $\phi = 10^\circ$  and almost all of the change in reflectance occur as  $\phi$  varies between  $\phi = 0^\circ$  to  $\phi = 30^\circ$ .

Figure 18 shows the variation in the reflectance with wavelength for the short wavelength. This Figure shows that as with the results reported for ZnO in the final report of NASA Grant NGR-05-009 very little energy is reflected for wavelength below 0.375 microns. This is probably due to the ZnO pigment used in the paints. The values shown in the Figures are not absolute since the detector did not intercept all of the source energy. However the ratio of the plotted reflectance of S-13G to Z-93 is approximately 1.00.

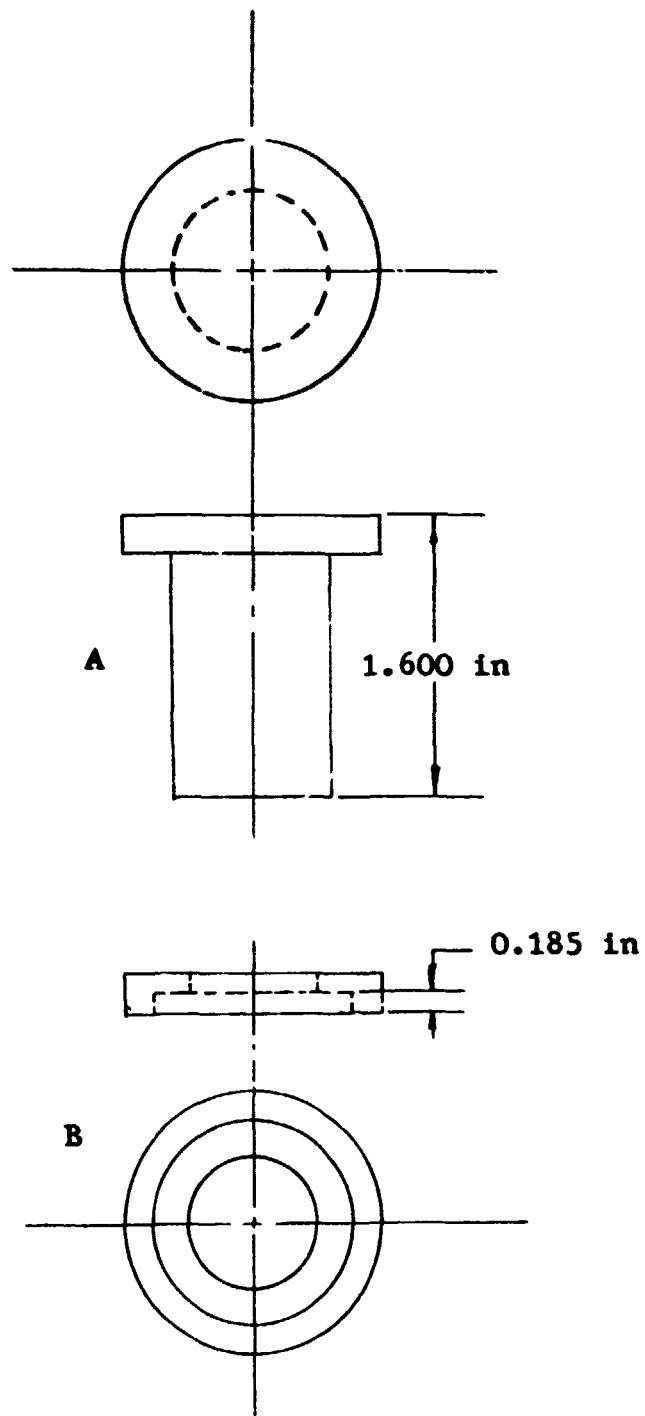


**Figure 1. Specimen Holder and Installation Device**



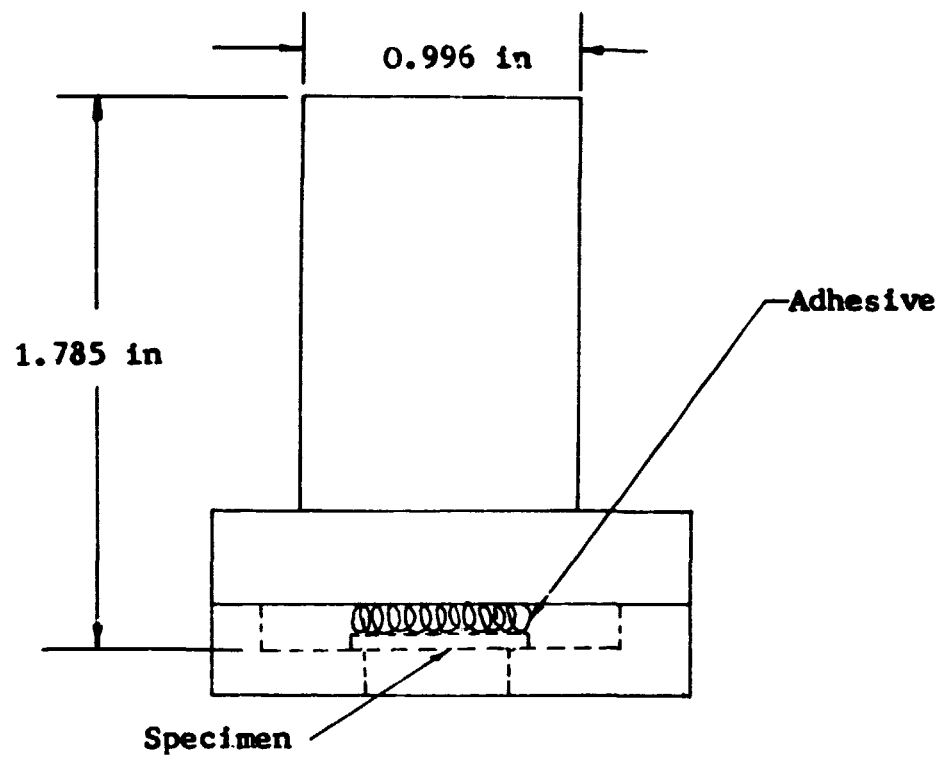


Figure 2. Specimen Installation

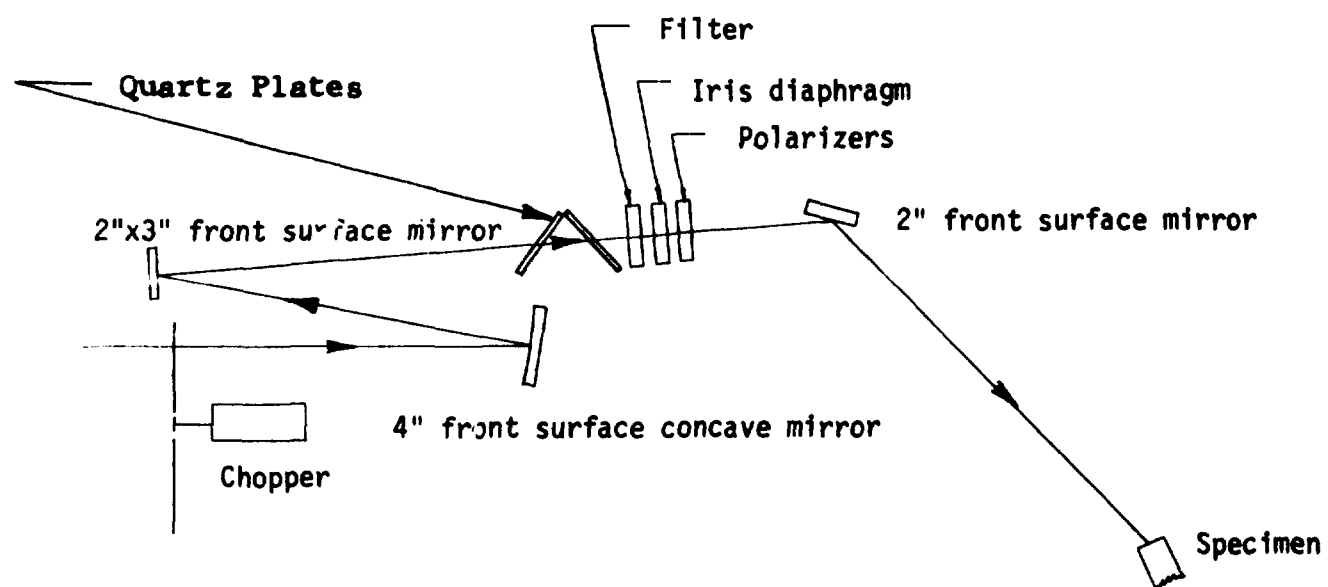


Figure 3. Schematic of Exit Optics

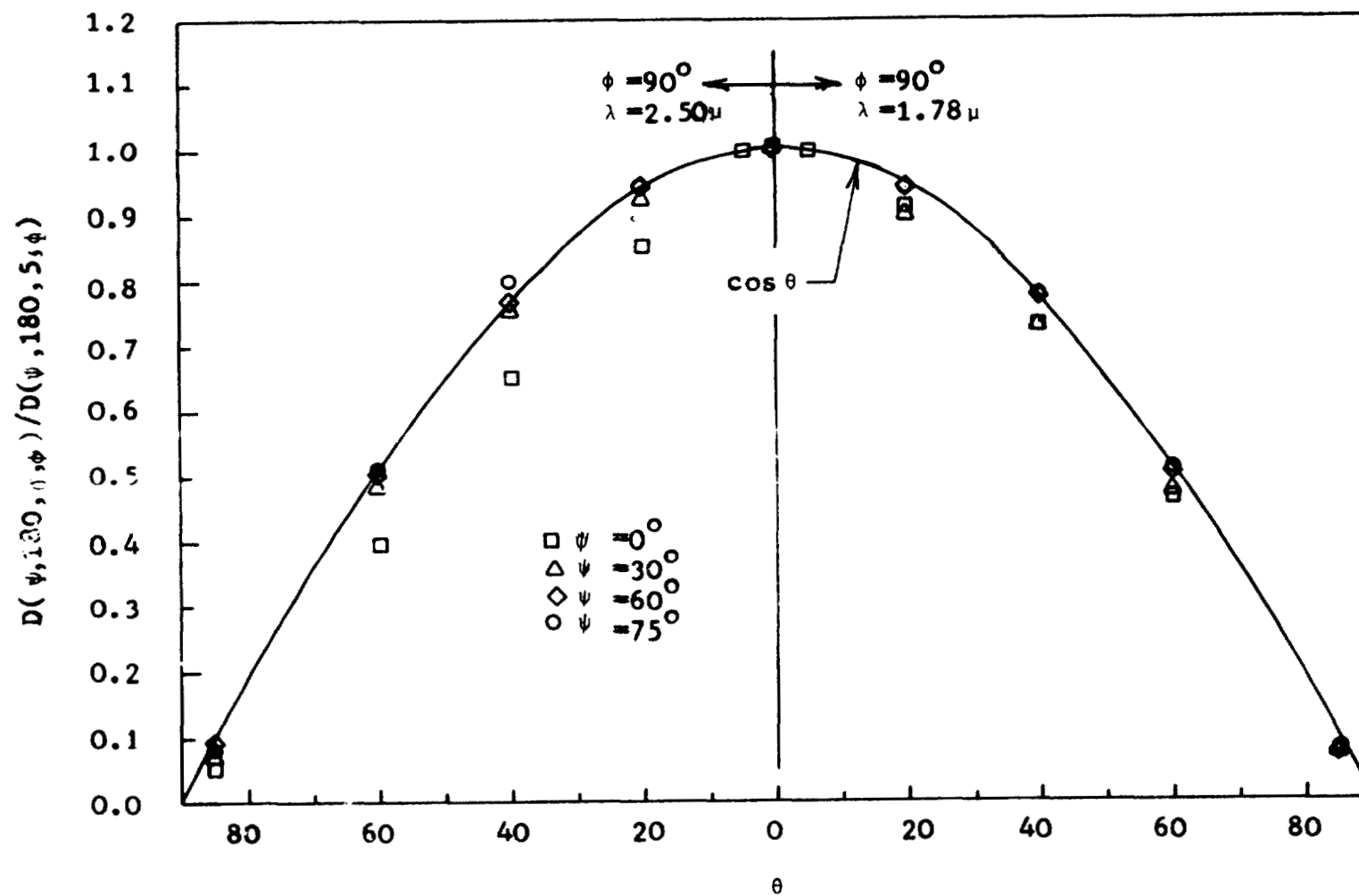


Figure 4. Reflectance of S-13G for  $\phi = 90^\circ$

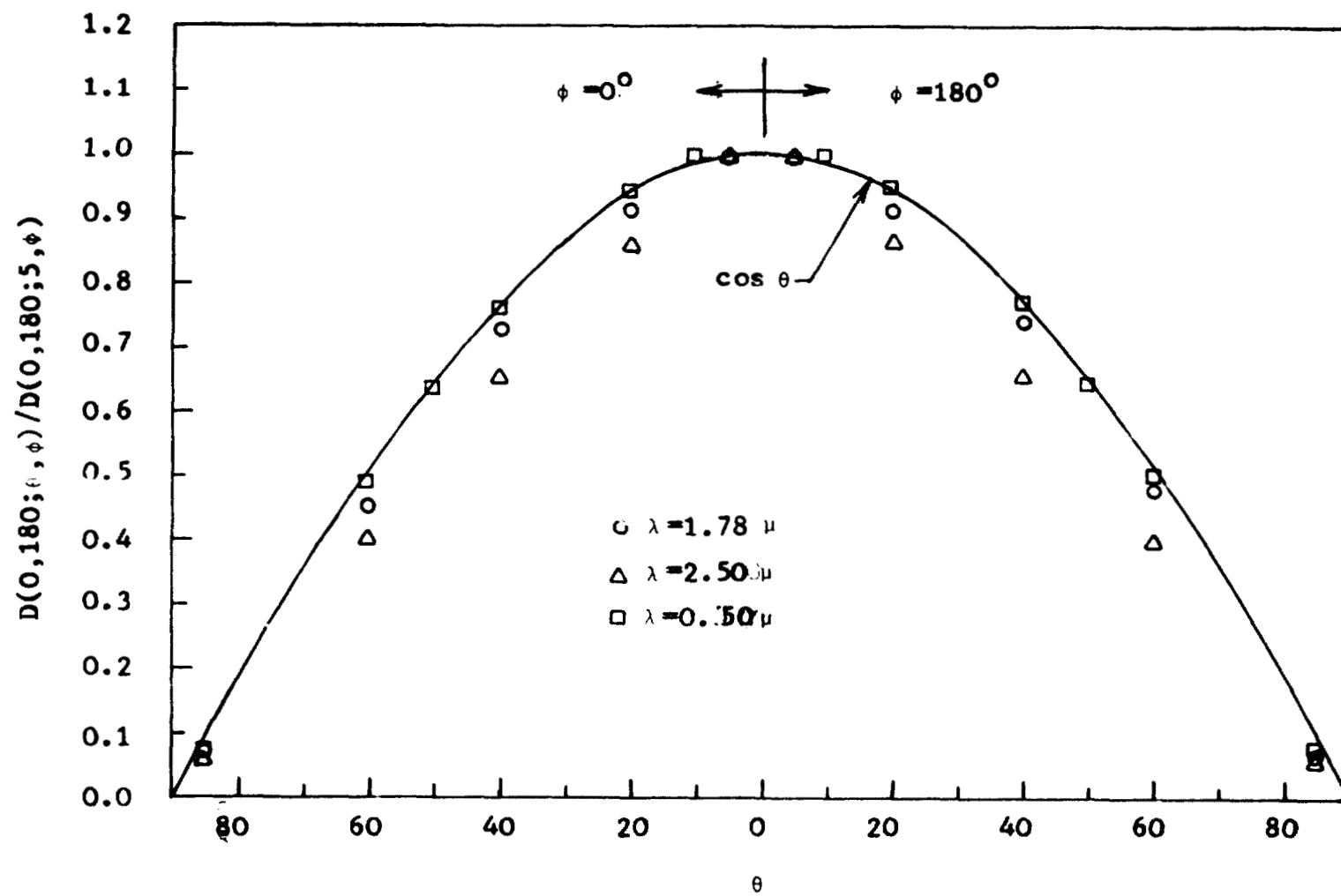


Figure 5. Reflectance of S-13G for  $\psi = 0^\circ$

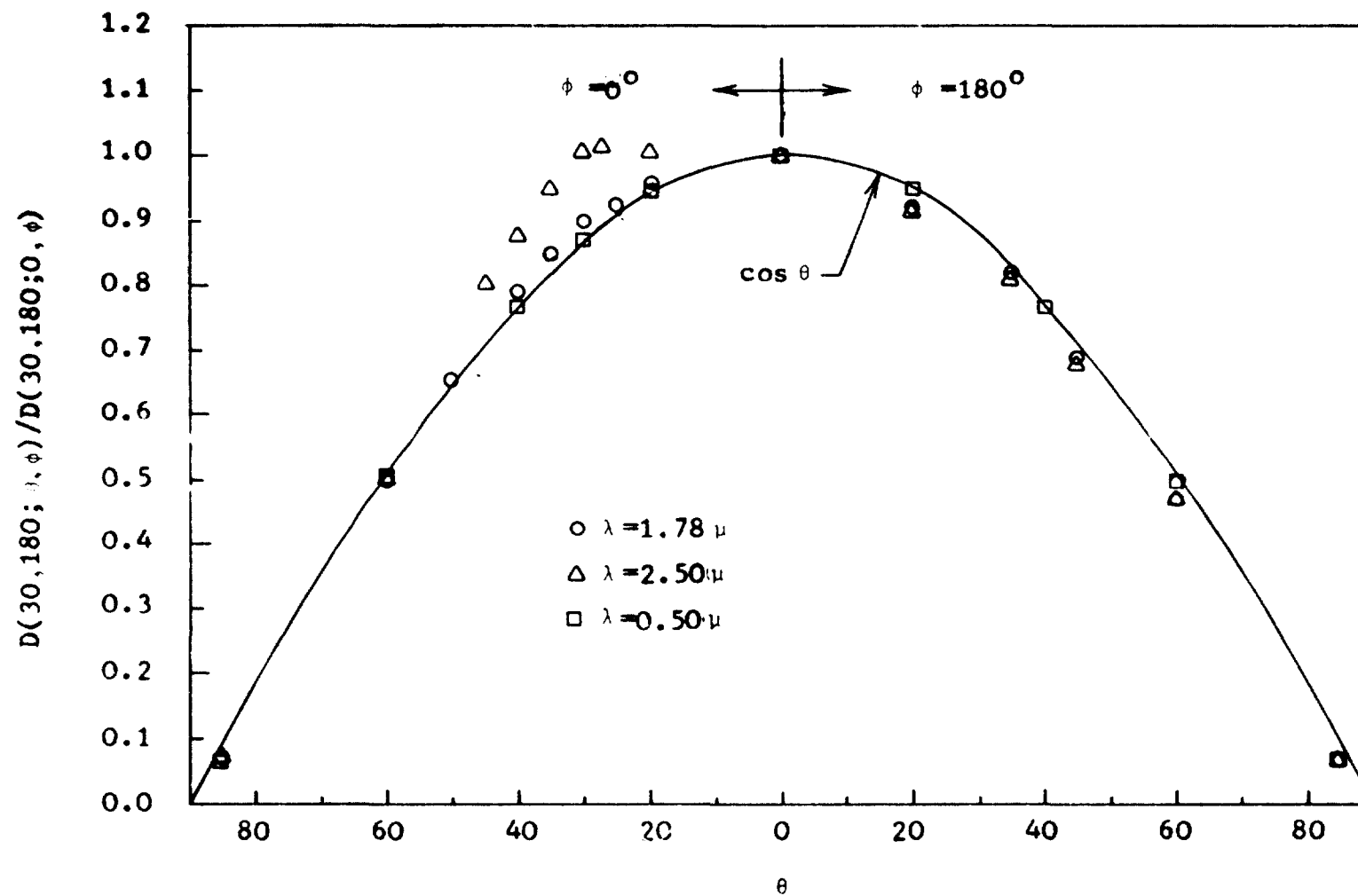


Figure 6. Reflectance of S-13G for  $\psi = 30^\circ$

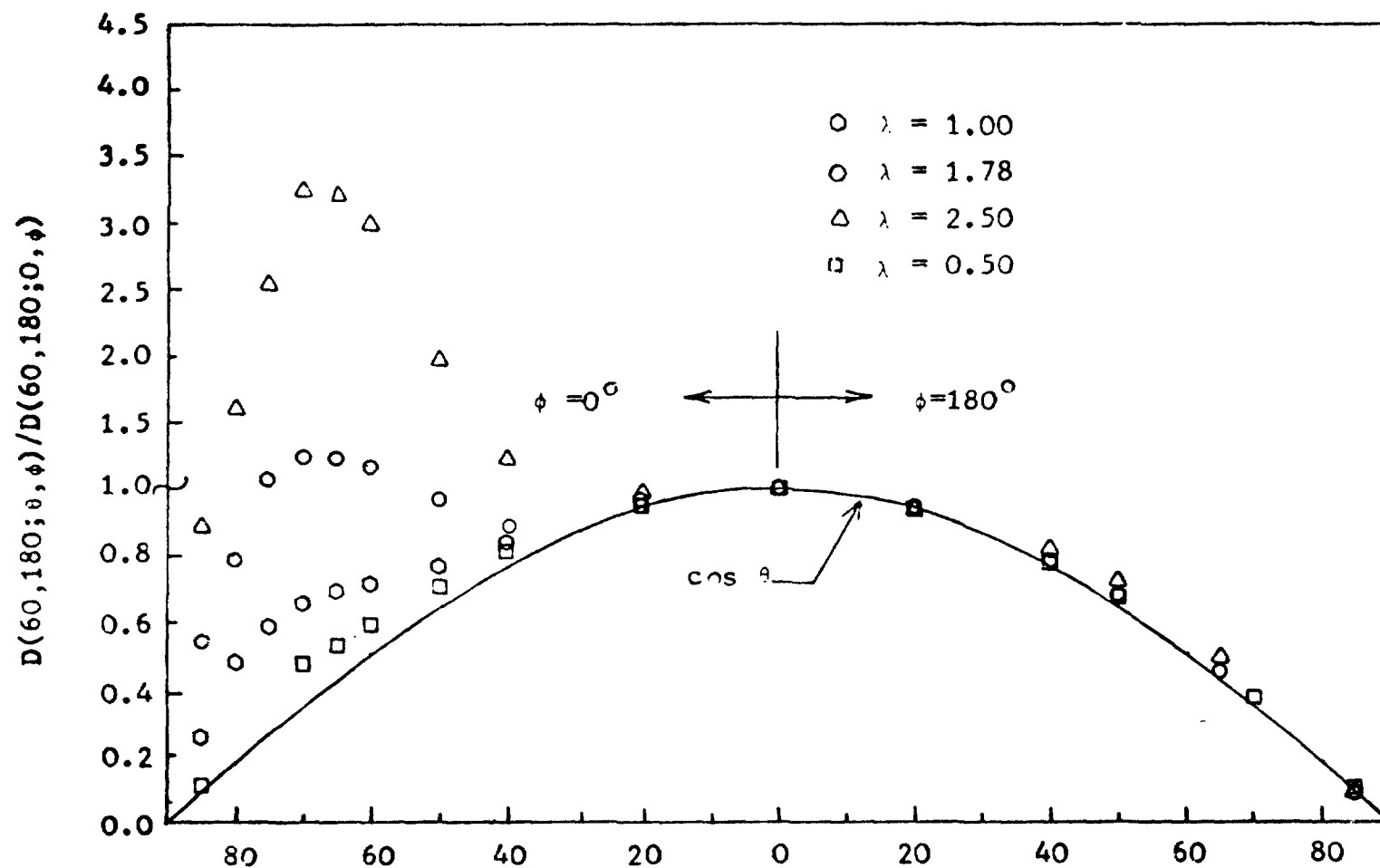


Figure 7. Reflectance of S-13G for  $\psi = 60^\circ$

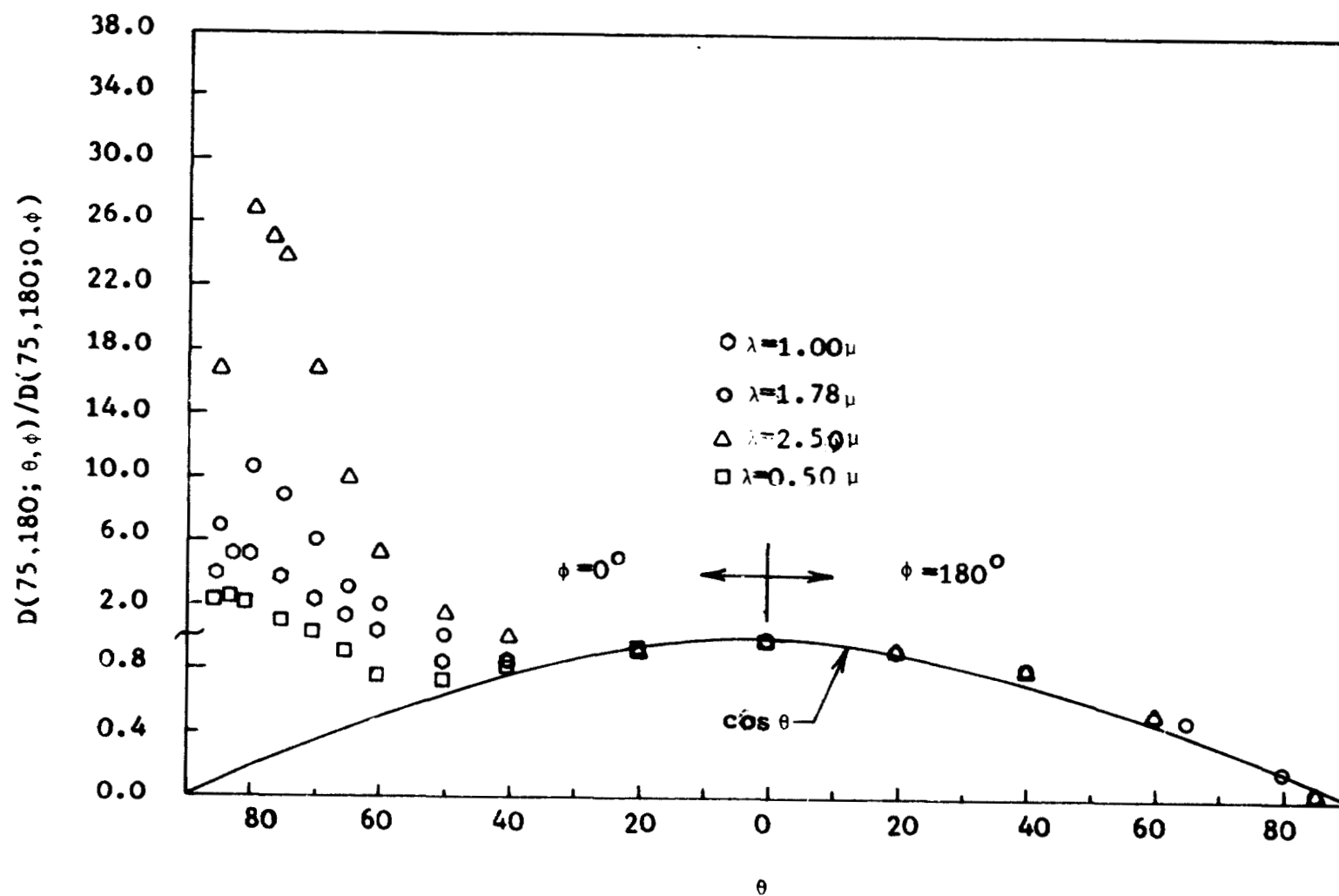


Figure 8. Reflectance of S-13G for  $\psi = 75^\circ$

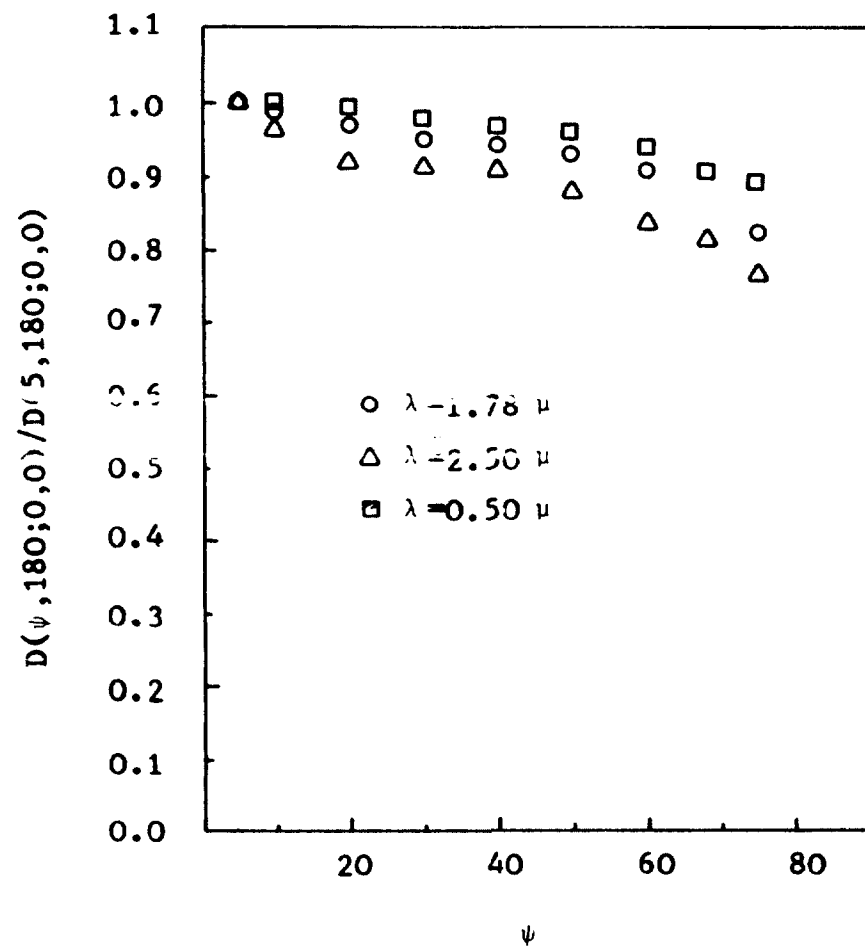


Figure 9. Variation of Reflectance with  $\psi$  for S-13G



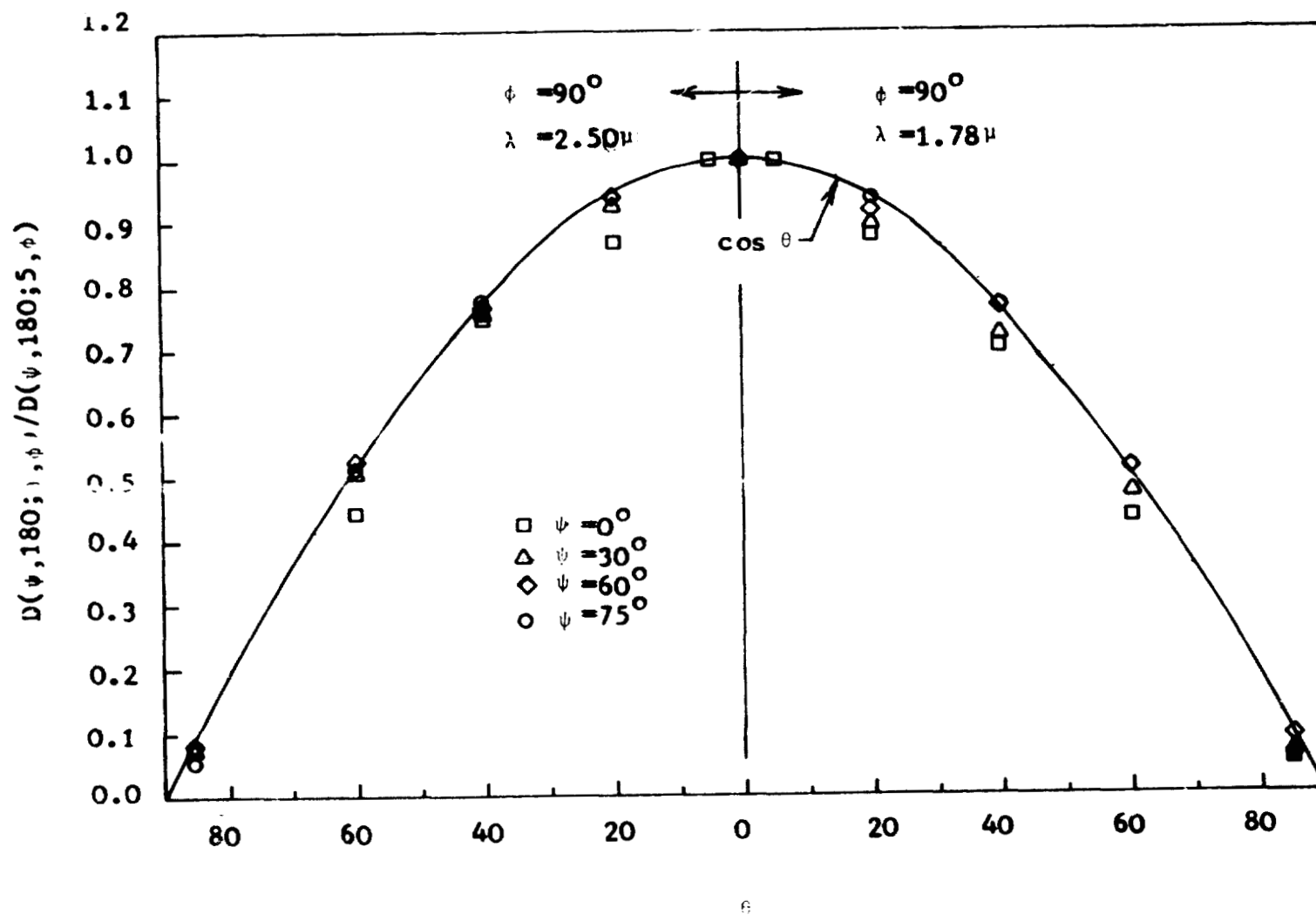


Figure 10. Reflectance of Z-93 for  $\phi = 90^\circ$

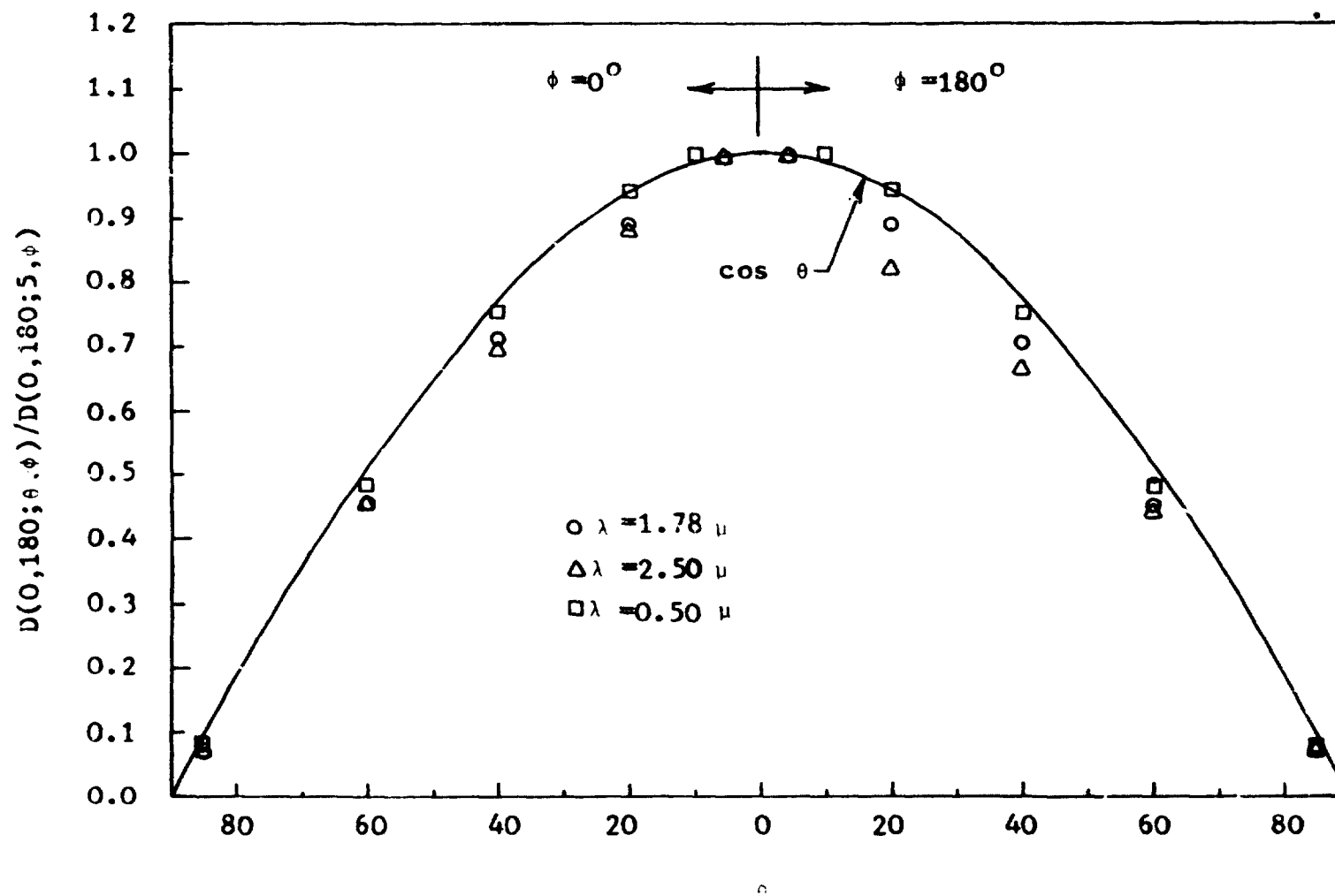


Figure 11. Reflectance of Z-93 for  $\psi = 0^\circ$

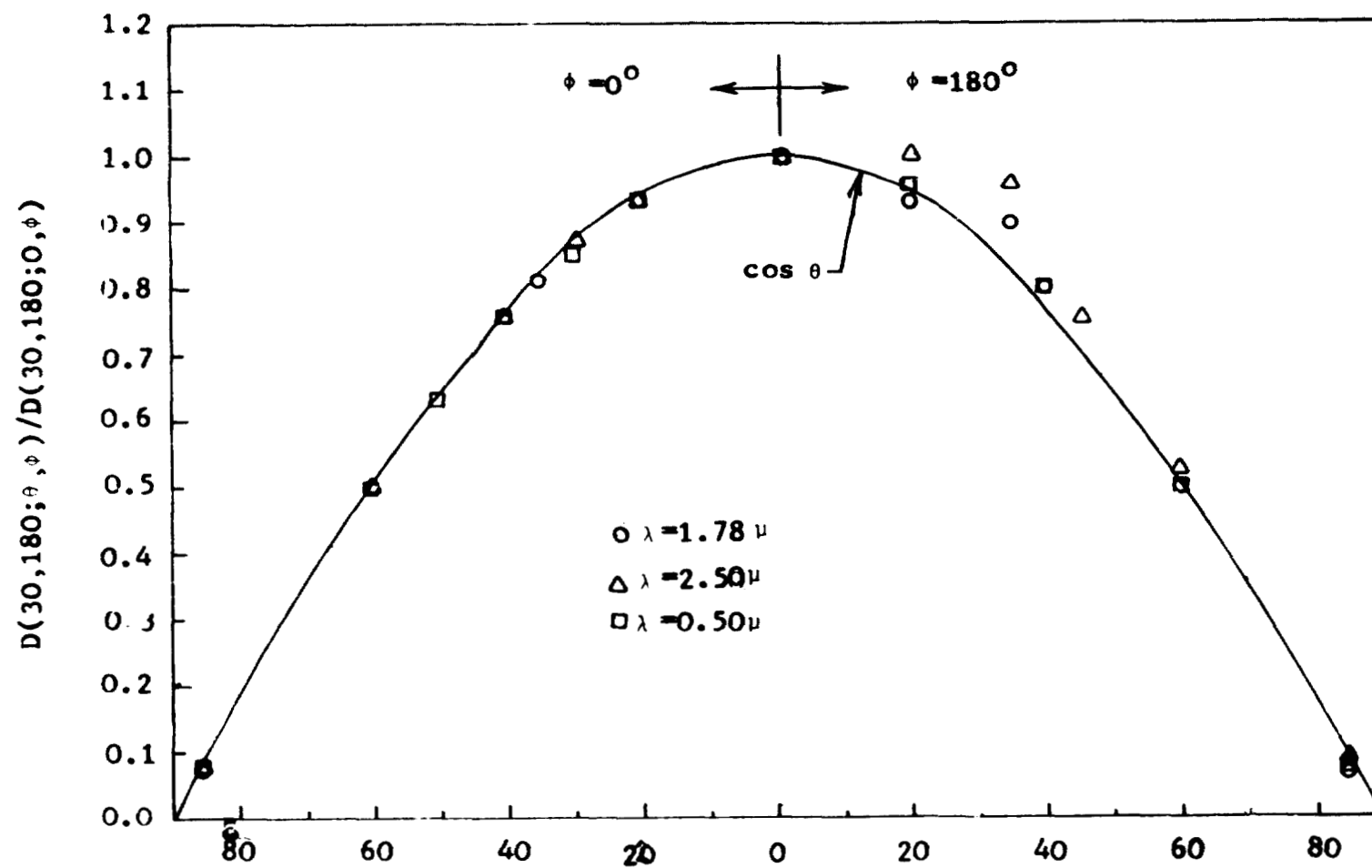


Figure 12. Reflectance of Z-93 for  $\psi = 30^\circ$

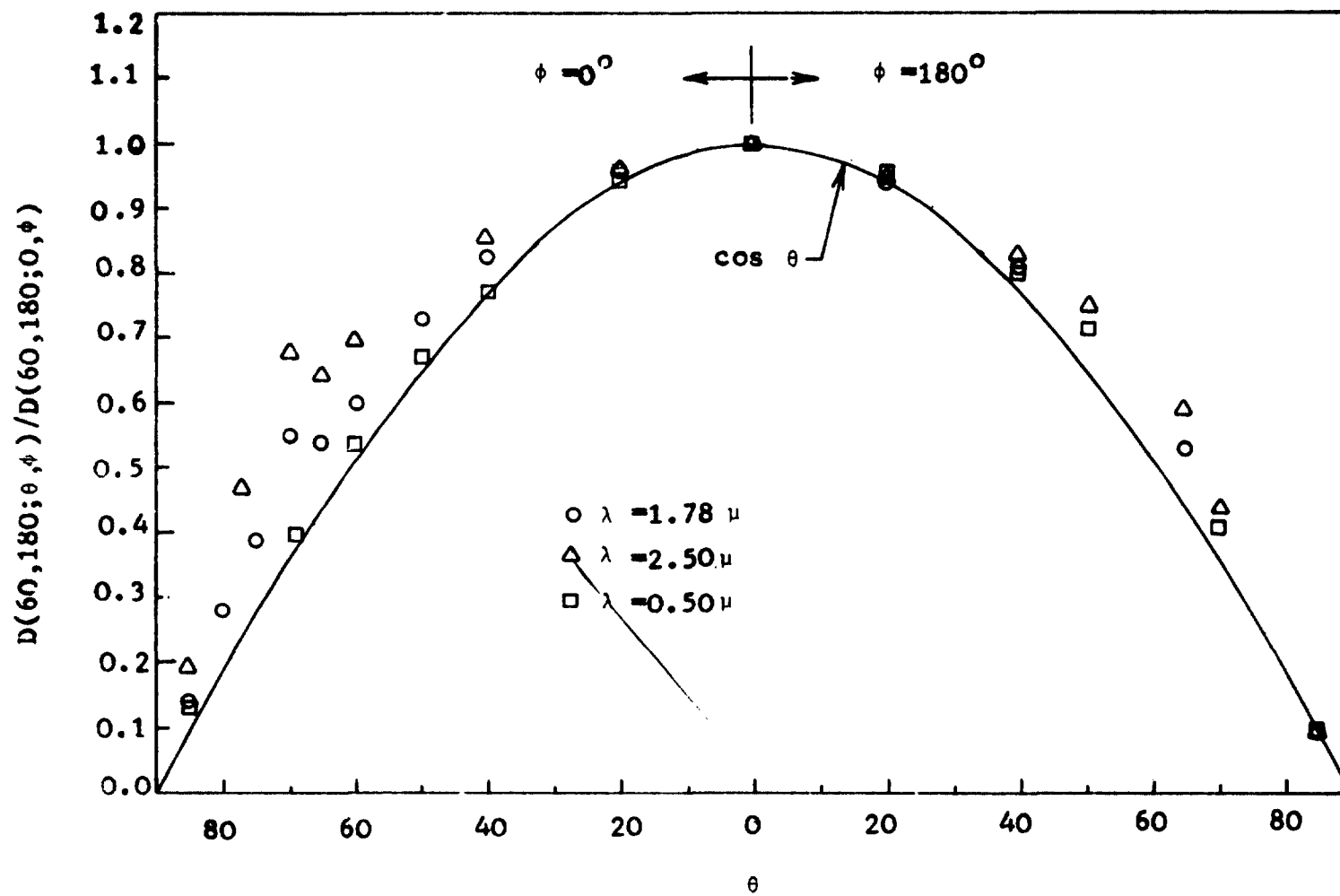


Figure 13. Reflectance of Z-93 for  $\psi = 60^\circ$

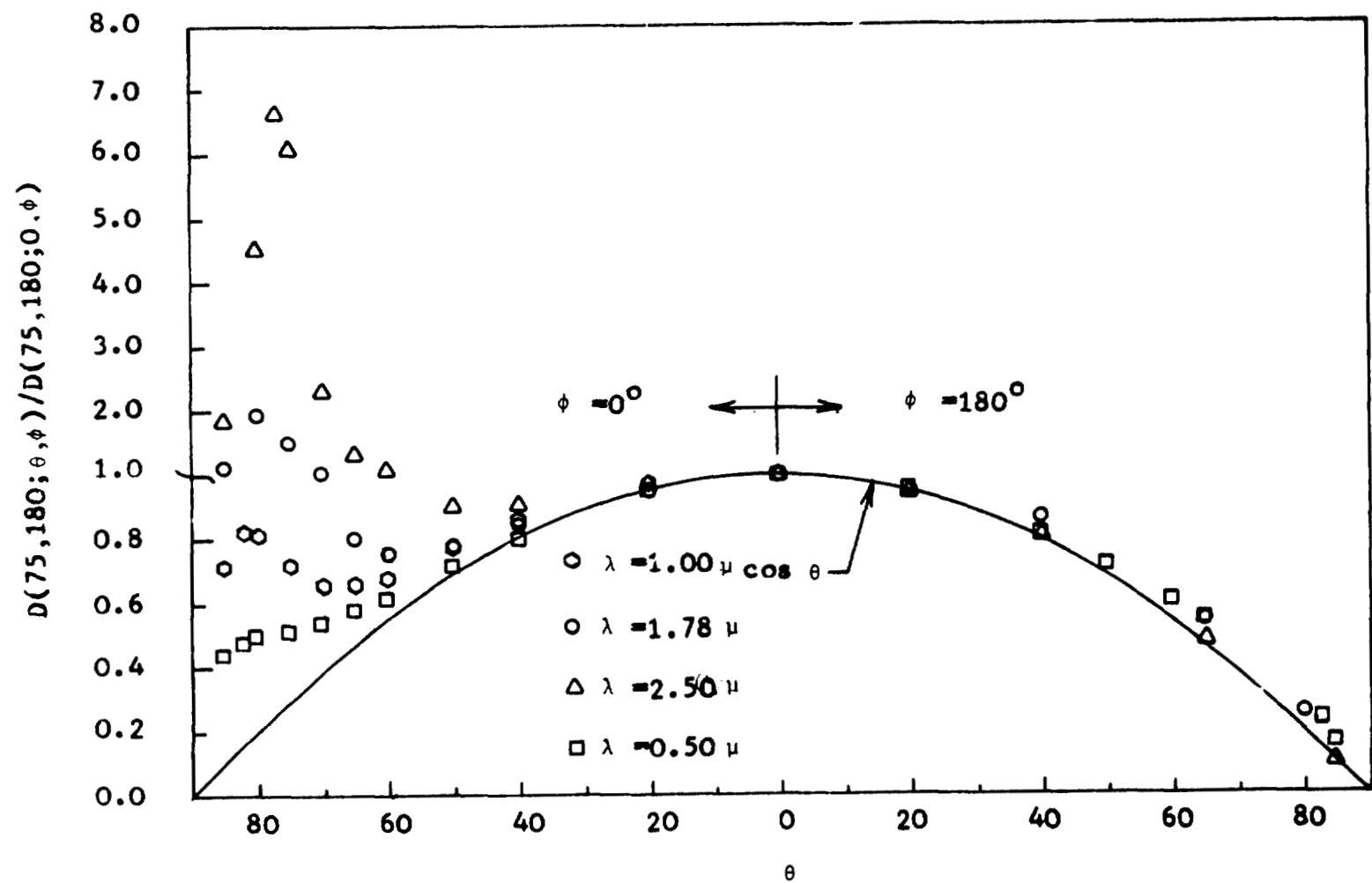


Figure 14. Reflectance of Z-93 for  $\psi = 75^\circ$

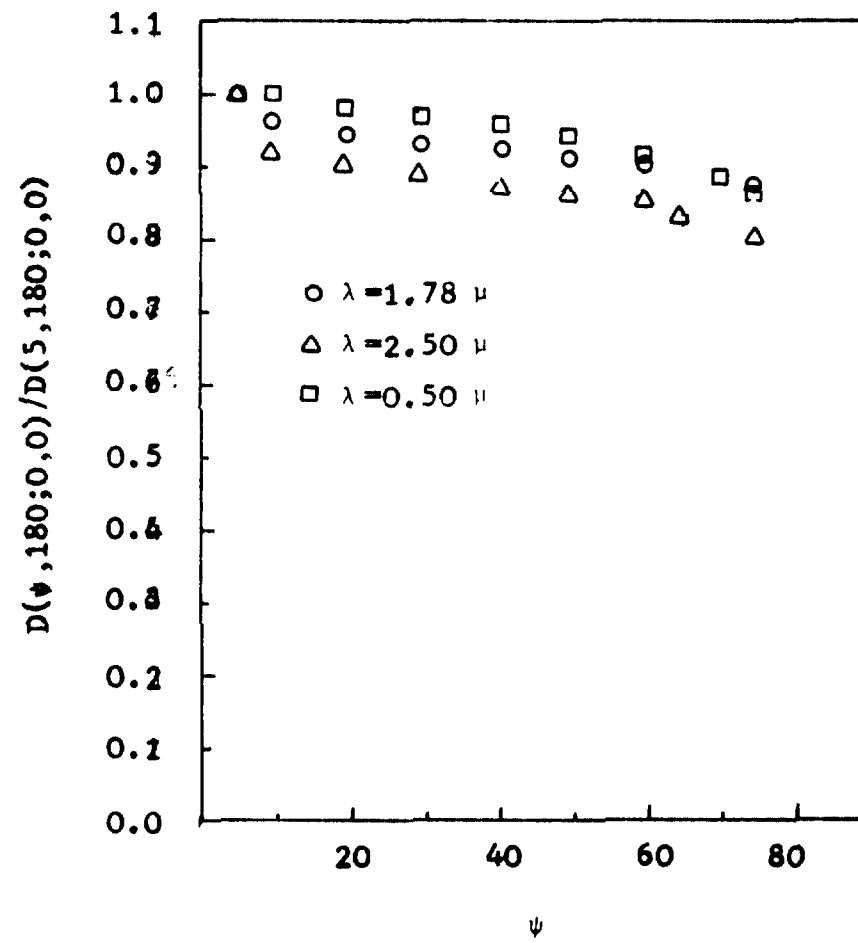


Figure 15. Variation of Reflectance of Z-93 With  $\psi$

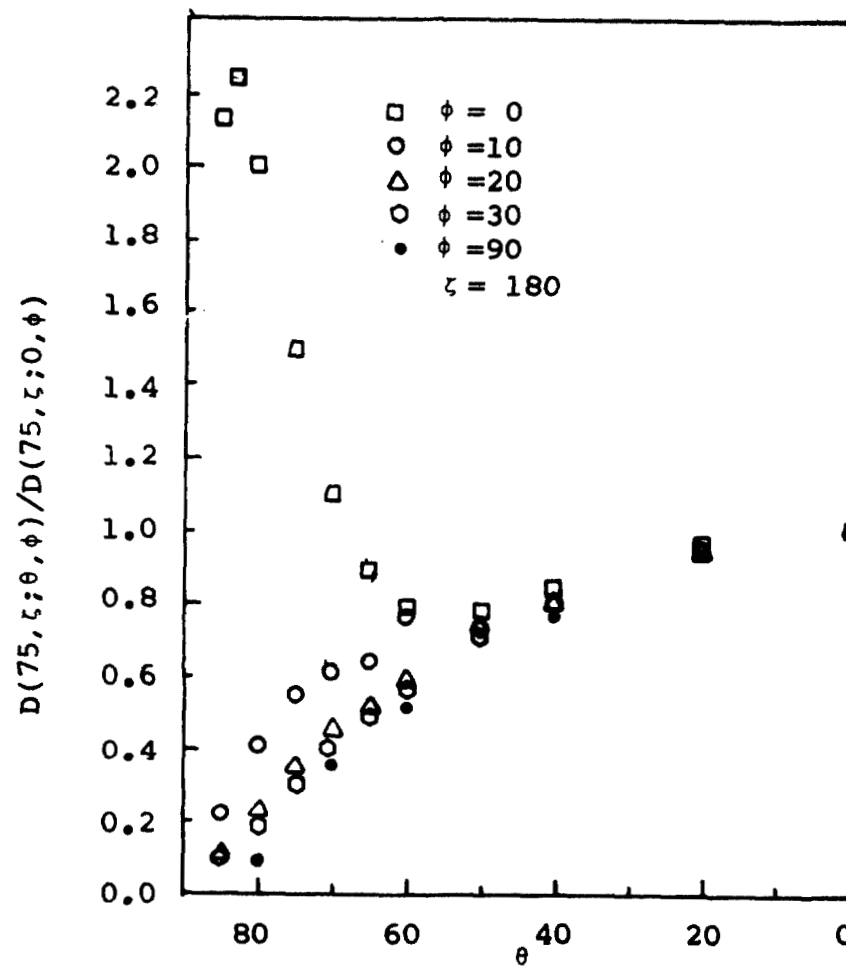


Figure 16. Variation of Reflectance with  $\phi$  for S-13G,  $\lambda = 0.500\mu$

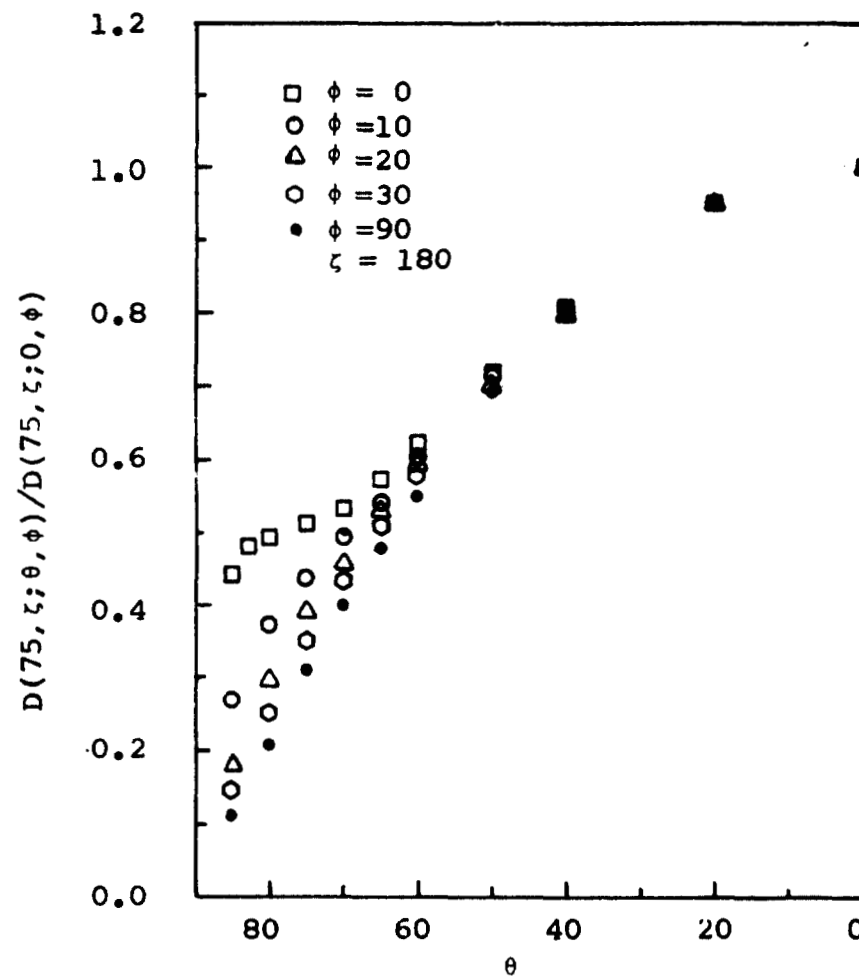


Figure 17. Variation of Reflectance with  $\phi$  for Z-93,  $\lambda = 0.500\mu$



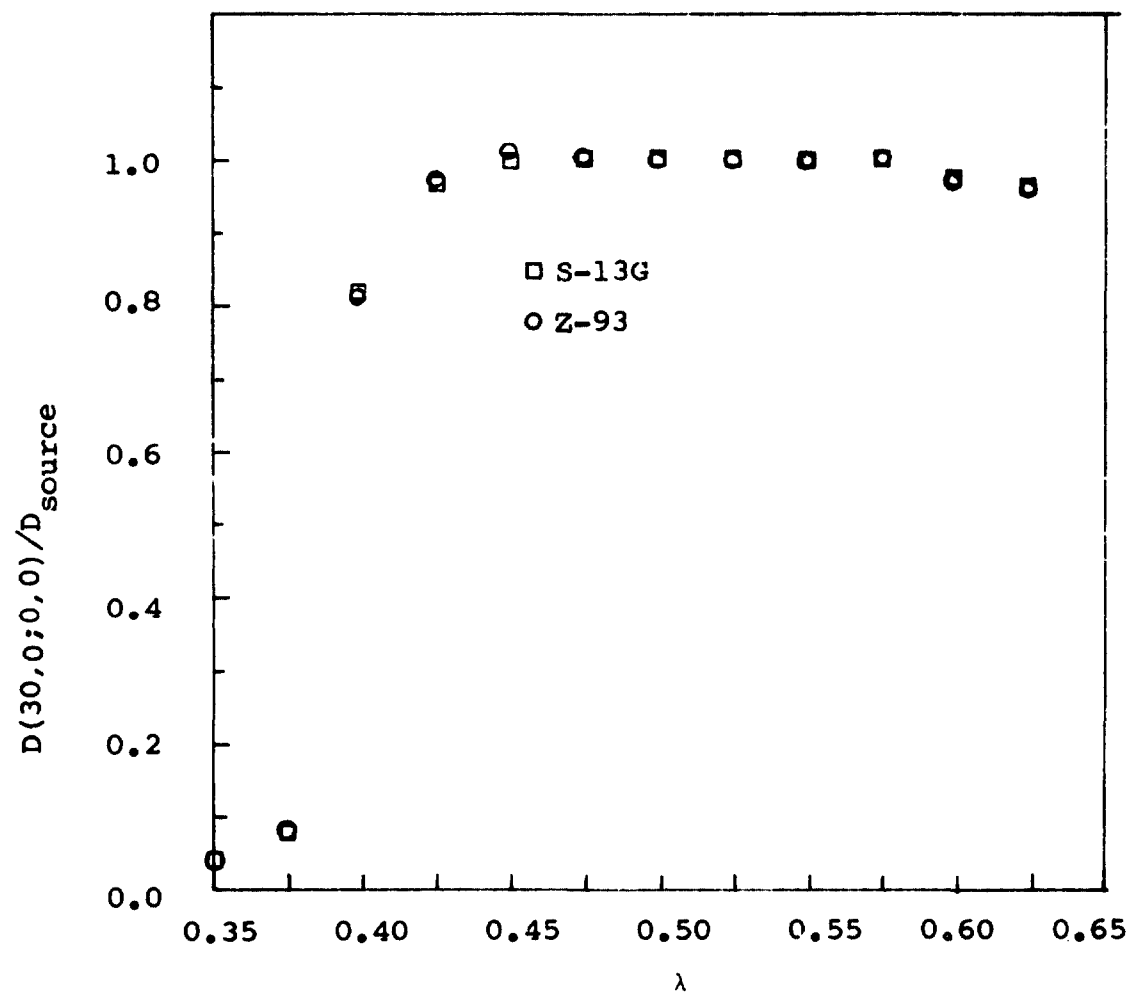


Figure 18. Variation of Reflectance with  $\lambda$  for S-13G and Z-93

TABLE 1  
VARIATION OF REFLECTANCE WITH SOURCE  
AND DETECTOR AZIMUTH  
(  $\lambda = 1.78, \theta = 0, \psi = 0$  )

<u><math>\phi</math></u>	<u><math>\zeta</math></u>	DETECTOR <u>S13-G</u>	DETECTOR <u>Z-93</u>
0	180	8.54	9.65
90	270	8.57	9.67
180	0	8.56	9.70
270	90	8.51	9.635
0	180	8.51	9.635

TABLE 2

REFLECTANCE OF S-13G AT 0.500 MICRONS  
 $D(0^\circ, 180^\circ; \theta, \phi) / D(0^\circ, 180^\circ; 5^\circ, \phi)$

<u><math>\theta</math></u>	<u><math>\phi=0^\circ</math></u>	<u><math>\phi=90^\circ</math></u>	<u><math>\phi=180^\circ</math></u>
10	1.000	1.000	1.000
20	0.947	0.948	0.947
40	0.761	0.766	0.767
50	0.634	0.641	0.640
60	0.487	0.495	0.497
85	0.077	0.080	0.085

TABLE 3

REFLECTANCE OF S-13G AT 1.78 MICRONS

$D(0^\circ, 180^\circ; \theta, \phi) / D(0^\circ, 180^\circ; 5^\circ, \phi)$

<u><math>\theta</math></u>	<u><math>\phi=0^\circ</math></u>	<u><math>\phi=90^\circ</math></u>	<u><math>\phi=180^\circ</math></u>	<u><math>\phi=270^\circ</math></u>
5	1.000	1.000	1.000	1.000
20	0.915	0.914	0.915	0.918
40	0.737	0.733	0.736	0.739
60	0.455	0.458	0.467	0.467
85	0.074	0.067	0.073	0.070

TABLE 4

REFLECTANCE OF S-13G AT 2.5 MICRONS

$$D(0^\circ, 180^\circ; \theta, \phi) / D(0^\circ, 180^\circ; 5^\circ, \phi)$$

<u><math>\theta</math></u>	<u><math>\phi=0^\circ</math></u>	<u><math>\phi=90^\circ</math></u>	<u><math>\phi=180^\circ</math></u>	<u><math>\phi=270^\circ</math></u>
5	1.000	1.000	1.000	1.000
20	0.853	0.852	0.865	0.856
40	0.651	0.649	0.663	0.648
60	0.409	0.404	0.406	0.412
85	0.052	0.063	0.064	0.064

TABLE 5

REFLECTANCE OF S-13G AT 0.500 MICRONS  
 $D(30^\circ, 180^\circ; \theta, \phi) / D(30^\circ, 180^\circ; 0^\circ, \phi)$

<u><math>\theta</math></u>	<u><math>\phi=0^\circ</math></u>	<u><math>\phi=90^\circ</math></u>	<u><math>\phi=180^\circ</math></u>
0	1.000	1.000	1.000
20	0.943	0.942	0.950
30	0.874	—	—
40	0.773	0.765	0.774
60	0.508	0.495	0.497
85	0.086	0.084	0.088

TABLE 6

REFLECTANCE OF S-13G AT 1.78 MICRONS  
 $D(30^\circ, 180^\circ; \theta, \phi) / D(30^\circ, 180^\circ; 0^\circ, \phi)$

<u><math>\theta</math></u>	<u><math>\phi=0^\circ</math></u>	<u><math>\phi=90^\circ</math></u>	<u><math>\phi=180^\circ</math></u>
0	1.000	1.000	1.000
20	0.956	0.906	0.918
25	0.931	—	—
30	0.896	—	—
35	0.848	—	0.822
40	0.788	0.730	—
45	—	—	0.689
50	0.654	—	—
60	0.498	0.468	0.472
85	0.071	0.069	0.073

TABLE 7

REFLECTANCE OF S-13G AT 2.5 MICRONS

$$D(30^\circ, 180^\circ; \theta, \phi) / D(30^\circ, 180^\circ; 0^\circ, \phi)$$

<u><math>\theta</math></u>	<u><math>\phi=0^\circ</math></u>	<u><math>\phi=90^\circ</math></u>	<u><math>\phi=180^\circ</math></u>
0	1.000	1.000	1.000
20	1.012	0.922	0.904
27	1.019	_____	_____
30	1.012	_____	_____
35	0.951	_____	0.829
40	0.879	0.746	_____
45	_____	_____	0.686
60	0.513	0.477	0.462
85	0.070	0.075	0.066



TABLE 8

REFLECTANCE OF S-13G AT 0.500 MICRONS  
 $D(60^\circ, 180^\circ; \theta, \phi) / D(60^\circ, 180^\circ; 0^\circ, \phi)$

<u><math>\theta</math></u>	<u><math>\phi=0^\circ</math></u>	<u><math>\phi=90^\circ</math></u>	<u><math>\phi=180^\circ</math></u>
0	1.000	1.000	1.000
20	0.951	0.945	0.941
30	0.899	—	—
40	0.804	0.769	0.782
50	—	—	0.671
60	0.588	0.503	—
65	0.530	—	—
70	0.474	0.342	0.374
85	0.205	0.086	0.105

TABLE 9

REFLECTANCE OF S-13G AT 1.78 MICRONS  
 $D(60^\circ, 180^\circ; \theta, \phi) / D(60^\circ, 180^\circ; 0^\circ, \phi)$

<u><math>\theta</math></u>	<u><math>\phi=0^\circ</math></u>	<u><math>\phi=90^\circ</math></u>	<u><math>\phi=180^\circ</math></u>
0	1.000	1.000	1.000
20	0.958	0.940	0.945
40	0.890	0.770	0.789
50	0.961	—	0.676
60	1.169	0.500	—
65	1.216	—	0.455
70	1.216	—	—
75	1.058	—	—
80	0.773	—	—
85	0.438	0.070	0.080

TABLE 10

REFLECTANCE OF S-13G AT 2.5 MICRONS  
 $D(60^\circ, 180^\circ; \theta, \phi) / D(60^\circ, 180^\circ; 0^\circ, \phi)$

<u><math>\theta</math></u>	<u><math>\phi=0^\circ</math></u>	<u><math>\phi=90^\circ</math></u>	<u><math>\phi=180^\circ</math></u>
0	1.000	1.000	1.000
20	0.983	0.940	0.968
40	1.230	0.770	0.822
50	1.980	—	0.726
60	2.990	0.500	—
65	3.200	—	0.492
70	3.220	—	—
75	2.540	—	—
80	1.660	—	—
85	0.880	0.090	0.085

TABLE 11

REFLECTANCE OF S-13G AT 0.500 MICRONS

$D(75^\circ, 180^\circ; \theta) / D(75^\circ, 180^\circ; 0^\circ, \phi)$

<u><math>\theta</math></u>	<u><math>\phi=0^\circ</math></u>	<u><math>\phi=90^\circ</math></u>	<u><math>\phi=180^\circ</math></u>
0	1.000	1.000	1.000
10	_____	_____	_____
20	0.961	0.943	0.944
40	0.840	0.764	0.783
50	0.786	_____	0.672
60	0.797	0.515	_____
65	0.887	_____	0.483
70	1.106	0.354	_____
75	1.507	_____	_____
80	2.070	_____	_____
83	2.247	_____	_____
85	2.143	0.088	0.131

TABLE 12

REFLECTANCE OF S-13G AT 1.78 MICRONS  
 $D(75^\circ, 180^\circ; \theta, \phi) / D(75^\circ, 180^\circ; 0^\circ; \phi)$

<u><math>\theta</math></u>	<u><math>\phi=0^\circ</math></u>	<u><math>\phi=90^\circ</math></u>	<u><math>\phi=180^\circ</math></u>
0	1.000	1.000	1.000
20	0.947	0.943	0.960
40	0.867	0.780	0.810
50	1.003	—	—
60	2.045	0.510	0.570
65	3.555	—	0.490
70	5.848	—	—
75	8.764	—	—
80	10.406	—	0.220
85	7.340	0.080	0.120

TABLE 13

REFLECTANCE OF S-13G AT 2.5 MICRONS  
 $D(75^\circ, 180^\circ; \theta, \phi) / D(75^\circ, 180^\circ; 0^\circ, \phi)$

<u><math>\theta</math></u>	<u><math>\phi=0</math></u>	<u><math>\phi=90</math></u>	<u><math>\phi=180</math></u>
0	1.000	1.000	1.000
20	0.948	0.942	0.950
40	1.056	0.795	0.810
50	1.763	—	—
60	5.415	0.515	0.270
65	9.961	—	—
70	6.996	—	—
75	23.914	—	—
80	27.274	—	—
85	17.471	0.077	0.110

TABLE 14  
VARIATION OF REFLECTANCE WITH  
SOURCE INCIDENT ANGLE  
 $D(\psi, 180^\circ; 0^\circ, 0^\circ) / D(5^\circ, 180^\circ; 0^\circ, 0^\circ)$   
S-13G

Incidence	Wavelength-microns		
<u>Angle</u>	<u>0.500</u>	<u>1.780</u>	<u>2.50</u>
5	_____	1.000	1.000
10	1.000	0.988	0.963
20	0.989	0.969	0.926
30	0.981	0.946	0.909
40	0.972	0.937	0.904
50	0.962	0.926	0.879
60	0.945	0.905	0.833
68	_____	_____	0.811
70	0.913	_____	_____
75	0.866	0.820	0.757

TABLE 15

REFLECTANCE OF Z-93 AT 0.500 MICRONS  
 $D(0^\circ, 180^\circ; \theta, \phi) / D(0^\circ, 180^\circ; 5^\circ, \phi)$

<u><math>\theta</math></u>	<u><math>\phi=0^\circ</math></u>	<u><math>\phi=90^\circ</math></u>	<u><math>\phi=180^\circ</math></u>
10	1.000	1.000	1.000
20	0.938	0.940	0.939
40	0.747	0.752	0.750
60	0.477	0.480	0.479
85	0.076	0.079	0.081



TABLE 16

REFLECTANCE OF Z-93 AT 1.78 MICRONS

$$D(0^{\circ}, 180^{\circ}; \theta, \phi) / D(0^{\circ}, 180^{\circ}; 5^{\circ}, \phi)$$

<u><math>\theta</math></u>	<u><math>\phi=0^{\circ}</math></u>	<u><math>\phi=90^{\circ}</math></u>	<u><math>\phi=180^{\circ}</math></u>	<u><math>\phi=270^{\circ}</math></u>
5	1.000	1.000	1.000	1.000
20	0.885	0.888	0.885	0.886
40	0.714	0.707	0.703	0.713
60	0.455	0.446	0.447	0.452
85	0.068	0.066	0.068	0.066

TABLE 17

REFLECTANCE OF Z-93 AT 2.5 MICRONS  
 $D(0^\circ, 180^\circ; \theta, \phi) / D(0^\circ, 180^\circ; 5^\circ, \phi)$

<u><math>\theta</math></u>	<u><math>\phi=0^\circ</math></u>	<u><math>\phi=90^\circ</math></u>	<u><math>\phi=180^\circ</math></u>	<u><math>\phi=270^\circ</math></u>
5	1.000	1.000	1.000	1.000
20	0.867	0.871	0.821	0.858
40	0.686	0.751	0.665	0.670
60	0.452	0.447	0.437	0.449
85	0.071	0.075	0.074	0.065

TABLE 18

REFLECTANCE OF Z-93 AT 0.500 MICRONS

$D(30^\circ, 180^\circ; \theta, \phi) / D(30^\circ, 180^\circ; 0^\circ, \phi)$

<u><math>\theta</math></u>	<u><math>\phi=0^\circ</math></u>	<u><math>\phi=90^\circ</math></u>	<u><math>\phi=180^\circ</math></u>
0	1.000	1.000	1.000
20	0.929	0.939	0.966
30	0.853	_____	_____
40	0.750	0.759	0.749
50	0.627	_____	_____
60	0.485	0.490	0.503
85	0.082	0.084	0.084

TABLE 19

REFLECTANCE OF Z-93 AT 1.78 MICRONS  
 $D(30^\circ, 180^\circ; \theta, \phi) / D(30^\circ, 180^\circ; 0^\circ, \phi)$

<u><math>\epsilon</math></u>	<u><math>\phi=0^\circ</math></u>	<u><math>\phi=90^\circ</math></u>	<u><math>\phi=180^\circ</math></u>
0	1.000	1.000	1.000
20	0.935	0.908	0.937
30	0.862	0.842	—
35	0.819	—	0.906
40	0.764	0.737	0.804
60	0.502	0.482	0.499
85	0.704	0.705	0.705

TABLE 20

REFLECTANCE OF Z-93 AT 2.5 MICRONS  
 $D(30^\circ, 180^\circ; \theta, \phi) / D(30^\circ, 180^\circ; 0^\circ, \phi)$

<u><math>\theta</math></u>	<u><math>\phi=0^\circ</math></u>	<u><math>\phi=90^\circ</math></u>	<u><math>\phi=180^\circ</math></u>
0	1.000	1.000	1.000
20	0.935	0.936	1.009
30	0.877	—	—
35	—	—	0.956
40	0.770	0.765	—
45	—	—	0.753
60	0.512	0.513	0.526
85	0.085	0.071	0.084

TABLE 21

REFLECTANCE OF Z-93 AT 0.500 MICRONS  
 $D(60^\circ, 180^\circ; \theta, \phi) / D(60^\circ, 180^\circ; 0^\circ, \phi)$

<u><math>\theta</math></u>	<u><math>\phi=0^\circ</math></u>	<u><math>\phi=90^\circ</math></u>	<u><math>\phi=180^\circ</math></u>
0	1.000	1.000	1.000
20	0.942	0.946	0.957
40	0.778	0.780	0.811
50	0.668	0.662	0.715
60	0.542	0.523	_____
70	0.396	0.363	0.411
85	0.128	0.097	0.105

TABLE 22

REFLECTANCE OF Z-93 AT 1.78 MICRONS  
 $D(60^\circ, 180^\circ; \theta, \phi) / D(60^\circ, 180^\circ; 0^\circ, \phi)$

<u><math>\theta</math></u>	<u><math>\phi=0^\circ</math></u>	<u><math>\phi=90^\circ</math></u>	<u><math>\phi=180^\circ</math></u>
0	1.000	1.000	1.000
20	0.951	0.917	0.944
40	0.812	0.783	0.811
50	0.730	_____	_____
60	0.608	0.522	_____
65	0.543	_____	0.529
70	0.547	_____	_____
75	0.388	_____	_____
80	0.279	_____	_____
85	0.144	0.085	0.091

TABLE 23

REFLECTANCE OF Z-93 AT 2.5 MICRONS  
 $D(60^\circ, 180^\circ; \theta, \phi) / D(60^\circ, 180^\circ; 0^\circ, \phi)$

<u><math>\theta</math></u>	<u><math>\phi=0^\circ</math></u>	<u><math>\phi=90^\circ</math></u>	<u><math>\phi=180^\circ</math></u>
0	1.000	1.000	1.000
20	0.961	0.940	0.948
40	0.863	0.772	0.832
50	_____	_____	0.755
60	0.693	0.535	_____
65	0.646	_____	0.589
70	0.680	_____	0.443
77	0.469	_____	_____
85	0.192	0.081	0.094



TABLE 24

REFLECTANCE OF Z-93 AT 0.500 MICRONS  
 $D(75^{\circ}, 180^{\circ}; \theta, \phi) / D(75^{\circ}, 180^{\circ}; 0^{\circ}, \phi)$

<u><math>\theta</math></u>	<u><math>\phi=0^{\circ}</math></u>	<u><math>\phi=90^{\circ}</math></u>	<u><math>\phi=180^{\circ}</math></u>
0	1.000	1.000	1.000
20	0.950	0.951	0.959
40	0.813	0.798	0.822
50	0.722	0.686	0.727
60	0.623	0.553	0.613
65	0.577	0.476	0.553
70	0.538	0.393	—
75	0.516	0.311	—
80	0.495	0.218	—
83	0.482	0.173	0.243
85	0.441	0.119	0.163

TABLE 25

REFLECTANCE OF Z-93 AT 1.78 MICRONS  
 $D(75^\circ, 180^\circ; \theta, \phi) / D(75^\circ, 180^\circ; 0^\circ, \phi)$

<u><math>\theta</math></u>	<u><math>\phi=0^\circ</math></u>	<u><math>\phi=90^\circ</math></u>	<u><math>\phi=180^\circ</math></u>
0	1.000	1.000	1.000
20	0.950	0.942	0.955
40	0.838	0.787	0.858
50	0.777	—	—
60	0.754	0.527	—
65	0.801	—	0.535
70	1.002	—	—
75	1.534	—	—
80	1.891	— —	0.262
85	1.084	0.072	—

TABLE 26  
REFLECTANCE OF Z-93 AT 2.5 MICRONS  
 $D(75^\circ, 180^\circ; \theta, \phi) / D(75^\circ, 180^\circ; 0^\circ, \phi)$

<u><math>\theta</math></u>	<u><math>\phi=0^\circ</math></u>	<u><math>\phi=90^\circ</math></u>	<u><math>\phi=180^\circ</math></u>
0	1.000	1.000	1.000
20	0.968	0.940	0.951
40	0.902	0.782	0.815
50	0.895	—	—
60	1.024	0.513	—
65	1.299	—	0.573
70	2.346	—	—
75	6.126	—	—
80	4.498	—	—
85	1.776	0.048	0.099

TABLE 27  
 VARIATION OF REFLECTANCE WITH  
 SOURCE INCIDENT ANGLE  
 $D(\psi, 180^\circ; 0^\circ, 0^\circ) / D(5^\circ, 180^\circ; 0^\circ, 0^\circ)$   
 Z-93

Incidence Angle	Wavelength-microns		
	<u>0.500</u>	<u>1.780</u>	<u>2.50</u>
5	_____	1.000	1.000
10	1.000	0.963	0.920
20	0.982	0.939	0.890
30	0.970	0.929	0.880
40	0.957	0.917	0.870
50	0.942	0.906	0.860
60	0.918	0.896	0.850
65	_____	_____	0.930
70	0.885	_____	_____
75	0.858	0.872	0.800

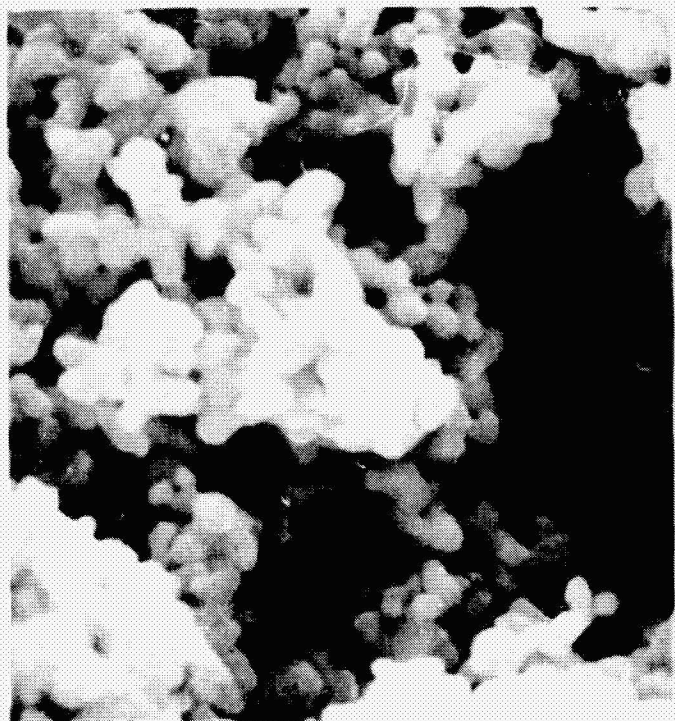
## APPENDIX

### Specimen Composition and Photographs

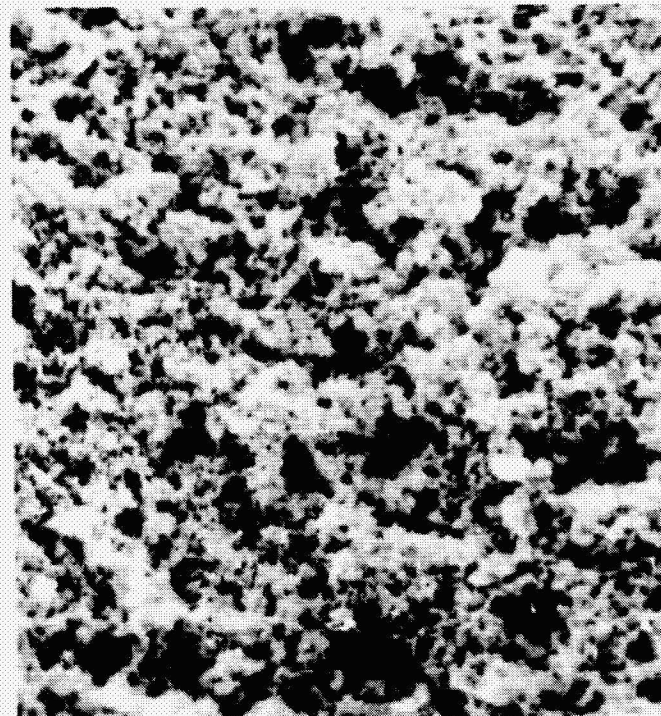
Z-93 is composed of a New Jersey Zinc SP500 Zinc Oxide pigment and a Sylvania Electric PS-7 Potassium Silicate binder. The pigment volume concentration (PVC) is 70%, and the sample thickness is 45 mil.

S13G is composed of a New Jersey Zinc SP Silicate treated Zinc Oxide pigment and a General Electric 602 Polydimetholeil-oxane binder. The PVC for S13G is 34% and the sample thickness of 7 mil.

**ORIGINAL PAGE IS  
OF POOR QUALITY**

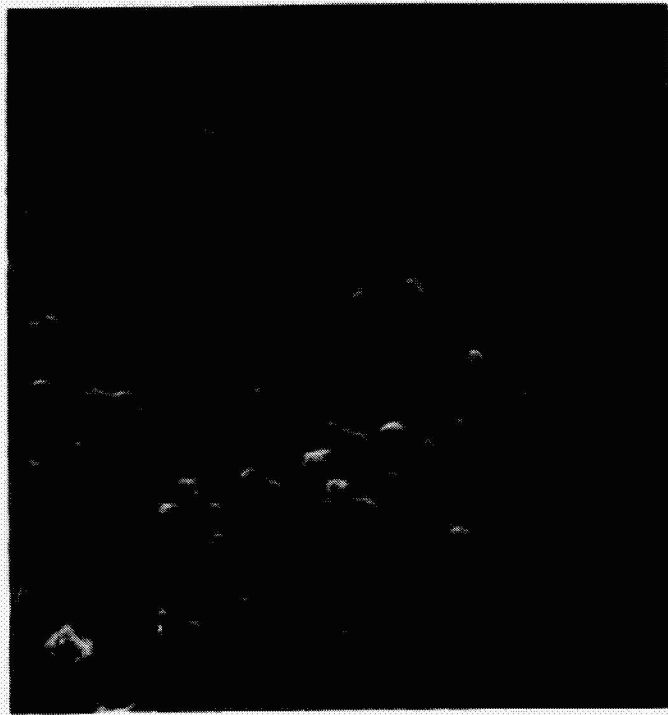


(a)



(b)

Figure A1. Photographs of Z-93: (a) 10K Magnification; (b) 1K Magnification



(a)



(b)

Figure A2. Photographs of S-13G: (a) 10K Magnification; (b) 1K Magnification